

# Allocating the environmental burdens in co-production of rare earth elements for EV magnets

Anders Nordelöf<sup>1, 2 \*</sup>, Anita Bongards<sup>3</sup>

\*Corresponding author: [anders.nordelof@vti.se](mailto:anders.nordelof@vti.se)

<sup>1</sup>The Swedish National Road and Transport Research Institute, Sweden

<sup>2</sup>Environmental Systems Analysis, Technology Management & Economics,  
Chalmers University of Technology, Sweden

<sup>3</sup>BorgWarner Stuttgart GmbH, Ludwigsburg, Germany

---

## Executive summary

Life cycle assessment (LCA) provides information for the environmental reporting of products containing rare earth elements (REEs). However, REEs occur jointly in mineral deposits, meaning that investigating rare earth oxides (REOs) that constitutes input to permanent magnet making for electric vehicle (EV) traction motors encompasses inherent methodological problem for LCA modelling – allocation of burdens between co-products. This study explores how the choice of modelled REO supply route and economic allocation between co-products impact on results for contributions to global warming in LCA of individual REOs relevant for EV magnet production, as well as for a full set of magnets for a typical electric motor of a passenger car. The study shows that the choice of REO supply route is the most important factor both for REO and motor results, while price variations influence results on the REO level. The effect of the economic allocation is minor on total motor results.

Keywords: Life cycle assessment | Allocation | Rare earth elements | Magnets | Electric motor

---

## 1 Introduction

Life cycle assessment (LCA) is playing an increasingly important role for government and company strategies. Meanwhile, the implementation of electric propulsion is taking place rapidly in all modes of transportation which reduces the transport sector's heavy reliance on fossil fuels. Still, it remains uncertain if this development is fast and comprehensive enough to mitigate the contributions of the sector to global warming, and avoid severe threats to society posed by climate change [1]. Electric powertrains are complex in terms of materials, and while they shift emissions away from the vehicle use phase, environmental trade-offs are found in the manufacturing of powertrain parts and the extraction of resources [2-4]. Permanent magnets in electric propulsion motors for electric vehicles (EVs) are one such example. Today's EV magnets typically contain rare earth elements (REEs), foremost neodymium, which gives high magnetic strength, and a smaller amount of dysprosium that contributes to the thermal stability of the magnet [5]. Two other REEs with relevance for the same magnet type are praseodymium, which can be mixed with the neodymium [6], and terbium, which is an alternative thermal stabilizer [7]. REEs are among the raw materials considered to be both critical and strategic for the automotive industry, as classified by the Critical Raw Materials Act of the European Union [8]. This act gives the European commission authority to set information requirements on the environmental reporting of REEs contained in permanent magnets [9]. Thus, being well-informed about the effects of inherent methodological challenges in the LCA modelling of the REE supply chain for EV magnets is very important for the automotive industry as well as European policy makers.

At present, economically viable production of REEs takes its starting point foremost in three types of mineral deposits – bastnäsite ore, monazite ore and ion adsorption clays [10]. In all of these, different REEs occur together in various combinations and grades, making them co-products [11]. Often there are also other metals present in the ore at the same site. For example, the world's largest REE production site in Bayan Obo in China primarily holds iron ore [10, 11]. However, due to their high values, REEs can be an important or even the main source of profit for a mineral production site, regardless of a lower mass output [11]. For all types of deposits, all processes treat the REE containing ores or concentrates jointly until the final solvent extraction where they are separated, typically as rare earth oxides (REOs), i.e., all the environmental burdens caused up to this point are shared between all the REOs produced. In LCA, this type of multi-output process poses a challenge for how to assign environmental burden between the different co-products, referred to as an allocation problem. In such cases, the ISO standard [12] for LCA states that when allocation cannot be avoided, the burdens shall be partitioned based on physical relationships, or when that is not sufficient, based on other relationships, for example in proportion to their economic value.

Further complicating this allocation problem, the production of REOs has a balancing problem [6], meaning that the demand for one or several of the co-products, for example neodymium for magnet production, leads to an over-supply of the others, as they end up being produced due to their presence in the deposit rather than in relation to their demand. In response, less profitable REOs are sometimes stockpiled [6], and non-profitable REOs might even be disposed [13]. Accordingly, even if physicochemical reaction-based and mass-based physical allocation is strived for, for example by Wang et al. [14], most existing LCA research, e.g. Koltun and Tharumarajah [10], Bailey et al. [13] and Zaimes et al. [15], agree that economic allocation is the recommended approach for the partitioning of the environmental burdens between co-produced REEs.

Another area of attention is inventory data availability and representativity for the different supply routes. Arshi et al. [16] criticizes the commercial LCA databases provided by Ecoinvent and Sphera for providing REO production data that it is inconsistent and old, and highly aggregated and non-transparent, respectively. However, relatively detailed inventory data is available, as exemplified by Vahidi and Zhao [17], Lee and Wen [18] and Schulze et al. [19]. In addition to this, first Bailey et al. [13] and then also Schreiber et al. [20] have scrutinized available literature data for the modelling of all steps from mining to individual REOs in several LCA studies and pointed out inconsistencies and gaps, before recommending how to best represent current state of the art processing procedures. But neither Bailey et al. [13], nor Schreiber et al. [20], explore the variation of results occurring in economic allocation or present results on the individual REO level.

Consequently, there is good reason to revisit the question of economic allocation in LCA studies of the REE supply chain, to provide better understanding of how, for example, price fluctuations influence LCA based reporting such as carbon footprints of magnets and even complete EV propulsion motors.

## 2 Purpose

This study investigates how the choice of modelled REO supply route and price variations among the co-products generated, influence on results for contributions to global warming in LCA of individual REOs relevant for EV magnet production, as well as for a complete set of magnets in the context of a typical electric motor (e-motor) for propulsion of a passenger car. The goal is to inform the EV industry about key challenges in sustainability reporting coupled to permanent magnets, and e-motors.

## 3 Methods

The LCA study takes an attributional approach and limits the technical system boundary to a cradle-to-gate scope, as the focus is set on the REE supply chain. Two different life cycle scopes quantify the burden of the product system at (1) the factory gate of REO production, and (2) the factory gate of electric motor manufacturing. For the second level, the share of burden caused by the magnets delivered to this factory is reported separately to illustrate how REO allocation procedure affects the result for the full set of magnets, as well as the complete e-motor. Data for two different REO supply routes are compared in two alternative foreground systems, mixed ore from the Bayan Obo open pit mine and a typical ion-adsorption clay deposit in Southern China. For full inventory analysis of each route, this data is combined with background data from the Ecoinvent version 3.10 database. Next, production of neodymium- and dysprosium-containing magnets

and the manufacturing of complete e-motors relevant for EV applications is modelled based on previous work by the main author [21-23].

As a first step, price data for all products coming out of the alternative REE supply routes for different time periods was collected, along with average data for the composition representative of the two different deposits. At the points in each supply chain where multiple products are output from the same process, a mass-economic allocation factor  $X_i$  of product  $i$  can then be calculated from its mass fraction  $C_i$  in the output and its price  $P_i$  as a commodity, and normalize this value over sum for all output products in that specific step:

$$X_i = \frac{C_i \cdot P_i}{\sum_{all} (C_i \cdot P_i)} \quad (1)$$

As can be noted, setting all prices to the same value, for example  $P_i = 1$ , gives the equation for the simpler mass-based allocation approach.

## 4 Modelling of rare earth oxides supply routes

### 4.1 Bayan obo mixed ore route

The Bayan Obo mine site consists of multiple orebodies which in turn are built up by a large amount of different minerals containing valuable REEs, iron, and niobium [24]. Jin et al. [25] report average ore grades of 6% REOs, 35% of iron oxides, and 0.13% of niobium oxide for the complete site. As a result of the variation between REE containing minerals in different parts of the orebodies, the nearby concentrating facilities typically handles a mixed raw ore input, with bastnäsite and monazite among the primary REE minerals [25].

The processing of the mixed ore to get individual REOs can be described in steps [13, 20]. The first is mining, to acquire raw ore, which is sent to the concentrating facilities. It is followed by physical beneficiation, like grinding and different methods for separation. At this stage, the REO concentrate is separated from the iron and niobium bearing ore concentrate. Next, the beneficiated REO concentrate is cracked in a roasting process and goes through several subsequent chemical process steps such as leaching, precipitation and solvent extraction to get substances containing individual REEs. In a finishing step, these are calcinated to output REOs. In this chain of events, ammonium chloride is generated as a by-product.

For the modelling of the Bayan Obo mixed ore route, the unit process data compilation by Bailey et al. [13] is taken as a starting point, which in turn foremost reports data from Lee and Wen [18], but also Zaimes et al. [15] and Sprecher et al. [26]. Bailey's datasets are updated with several corrections, due to inconsistencies or value revisions proposed by Schreiber et al. [20]. In the mining step, this includes an adjustment of the amount of energy consumed by the mining equipment, and an alignment of the ore composition with Lee and Wen [18] and Jin et al. [25]. The composition data selected is reported in Table 1.

In the beneficiation step, a coupled update concerns the REO, iron oxide and niobium oxide content in the concentrates based on the process efficiency reported by Lee and Wen [18, 27]. The amount of steam is also corrected in line with original source [18]. Furthermore, for the acid roasting and leaching steps, the data has been swapped from relying on Sprecher et al. [26] to Lee and Wen [18], again because of the change of concentrate composition in the preceding step. However, since Schreiber et al. [20] identify that the value provided by Lee and Wen [18] for the roasting energy consumption is an outlier compared to other studies, it was updated based on a later publication by Lee and Wen [27], and is now in accordance with the Chinese 2016-2020 rare earths industry development plan.

### 4.2 Ion-adsorption clay deposit route

The ion-adsorption clay deposits, also known as ionic clays, occur in Southern China [19, 28]. In these deposits the REE form ions which are adsorbed to aluminosilicate clay particles [19]. The most common way to extract them is in-situ leaching [20]. The ore grade is generally low, about 0.05–0.5% REO, and current mines in operation are typically in the range of 0.2–0.4% [19]. However, the share of heavy REEs, for example terbium and dysprosium, is relatively high.

Table 1: Fractions of different REOs in relation to total REO content included in the studied ore types.

|                    |                                 | Bayan Obo mixed ore | Ionic clay ore |
|--------------------|---------------------------------|---------------------|----------------|
| Lanthanum oxide    | La <sub>2</sub> O <sub>3</sub>  | 23.1%               | 27.8%          |
| Cerium oxide       | CeO <sub>2</sub>                | 50.2%               | 3.4%           |
| Praseodymium oxide | Pr <sub>6</sub> O <sub>11</sub> | 6.2%                | 5.9%           |
| Neodymium oxide    | Nd <sub>2</sub> O <sub>3</sub>  | 18.6%               | 17.7%          |
| Europium oxide     | Sm <sub>2</sub> O <sub>3</sub>  | 0.8%                | 0.9%           |
| Gadolinium oxide   | Eu <sub>2</sub> O <sub>3</sub>  | 0.2%                | 6.0%           |
| Samarium oxide     | Gd <sub>2</sub> O <sub>3</sub>  | 0.7%                | 4.6%           |
| Terbium oxide      | Tb <sub>4</sub> O <sub>7</sub>  | 0.1%                | 0.7%           |
| Dysprosium oxide   | Dy <sub>2</sub> O <sub>3</sub>  | 0.1%                | 3.7%           |
| Holmium oxide      | Ho <sub>2</sub> O <sub>3</sub>  | -                   | 0.7%           |
| Erbium oxide       | Er <sub>2</sub> O <sub>3</sub>  | -                   | 2.5%           |
| Thulium oxide      | Tm <sub>2</sub> O <sub>3</sub>  | -                   | 0.3%           |
| Ytterbium oxide    | Yb <sub>2</sub> O <sub>3</sub>  | -                   | 1.1%           |
| Lutetium oxide     | Lu <sub>2</sub> O <sub>3</sub>  | -                   | 0.2%           |
| Yttrium oxide      | Y <sub>2</sub> O <sub>3</sub>   | -                   | 24.4%          |

Note: Scandium is commonly also classified as a REE but not present in any of the investigated deposits.

The first step in the extraction of REEs from ionic clays is to prepare the site by drilling holes in the ore body where leachate can be injected [19]. RE ions are exchanged with ammonium ions [20]. The leaching solution is pumped into ponds and undergo precipitation to remove impurities and extract REEs into a concentrate with relatively high purity (91–93%), often in the form of a rare earth carbonate mix that is converted into a REO mix through a calcination step [20]. The concentrate is then sent to a solvent extraction process, which outputs individual REOs after additional precipitation and calcination [19].

For the ionic clay route, Bailey et al. [13] was again used as the starting point. These datasets combine information provided by Vahidi and Zhao [17], and Schulze et al. [19]. However, where Schulze et al. [19] presents unit process data for one low and one high ore grade, Bailey et al. [13] establish an average. This approach is retained in this study, but the ore composition in Schulze et al. [19] is aggregated for the share of several less common heavy REEs. Here, they have been disaggregated to individual REOs using the original underlying source [29]. The reason is that also these minor constituents are included in this study in terms of price data and allocation factors. The composition is reported in Table 1.

Another important note is that a part of the solid waste displaying low grade radioactivity is modelled as being deposited in connection to the concentration facility and not sent to more advanced treatment for radioactive material. This is in line with typical management of waste containing naturally occurring radioactive material as described by Qifan et al. [30] and Waggitt [31]. Based on Marx et al. [32], it is assumed to be non-reactive and proxied to behave as a non-sulfidic tailing. Finally, a faulty reporting of aluminum ion emissions was corrected to ammonium ion emissions, based on Schreiber et al. [20].

#### 4.3 Magnet and motor production

Permanent magnet fabrication for EVs is a powder metallurgical process where neodymium typically is added as a metal or an alloy [23, 33]. This means that neodymium oxide must be subject to a reduction process to form a metal before entering. Subsequently, it is blended into a mother alloy for magnet making containing electrolytic iron and boron in compound form [23]. The process involves many steps, including milling, pressing and sintering. Dysprosium is added as milled oxide powder and electrodeposited onto the surface of the sintered magnet base body. It is then subject to successive heat treatments, and the dysprosium diffuses into the neodymium rich phase between the grains of the magnet body, referred to as grain boundary diffusion [23, 33]. A surface protection layer of nickel is applied before magnetization. Readymade magnets are then only one of many components supplied to the e-motor assembly factory, along with electrical steel sheets, enameled copper wire, aluminum housing parts and several other inputs.

The modelling of neodymium-dysprosium-iron-boron magnets suitable for EV e-motors, and the production of them in China, along with subsequent shipping to Europe, is based on a complete permanent magnet synchronous machine inventory data model that also covers the production the magnet supply chain [21-23]. The total mass of this e-motor is 44.9 kg whereof 1.26 kg (2.8%) are magnets. 26% and 4% of the magnet body consist of neodymium and dysprosium, respectively. The peak power rating of the e-motor is 100 kW. Further electrical, geometrical, mass and operation data on this e-motor can be found in Nordelöf et al. [5]. In this study, the e-motor production is placed in an average European context.

## 5 Analysis of REO price data variation and allocation factors

Economic allocation based on price data for REEs presents several challenges. These include market price volatility and challenges in acquiring data. The prices of REEs are subject to significant fluctuations due to supply and demand dynamics, geopolitical factors, and market speculation. In terms of data collection, instantaneous trading prices for REOs are relatively easy to find, but free or easy access to historical price data is very limited. Ideally, price data for all co-products of the product system should come from one single coherent source. Figure 1 shows the monthly price variation in percent for lanthanum oxide and the REOs most relevant for traction motor magnets – neodymium oxide, praseodymium oxide, dysprosium oxide and terbium oxide – as well as iron ore and niobium oxide, in relation to each individual commodity's price in January 2021. An example of month-to-month price volatility, terbium oxide shifted down with 28% from May to June 2021.

Catena-X is a data ecosystem designed to exchange LCA data between different tiers of the supply chain of the automotive industry. It's product carbon footprint rulebook [34] builds on the ISO standard for LCA [12]. This rulebook aims to increase consistency of automotive carbon footprints and specifies that if the ratio of economic values of co-products is greater than five, economic allocation should be applied. Table 2 reports the yearly average prices for same REOs, iron ore and niobium oxide, as in Figure 1, but now normalized to the price for lanthanum oxide. Table 2 shows that the normalized price for typical EV magnet REOs ranges between 83 and 2020 for the yearly averages during 2021–2024. Comparing Figure 1 and Table 2, it can be noted that averaging over a 12-month period effectively mitigates most of the extreme price fluctuations. However, Table 2 still indicates that prices of a single REO can exhibit significant annual variability.

Catena-X [34] recommends that price data is averaged over 3–5 years to smoothen out these fluctuations. Other literature, e.g. Santero and Hendry [35], recommend an even longer time period for averaging prices in economic allocation of metals, 10 years.

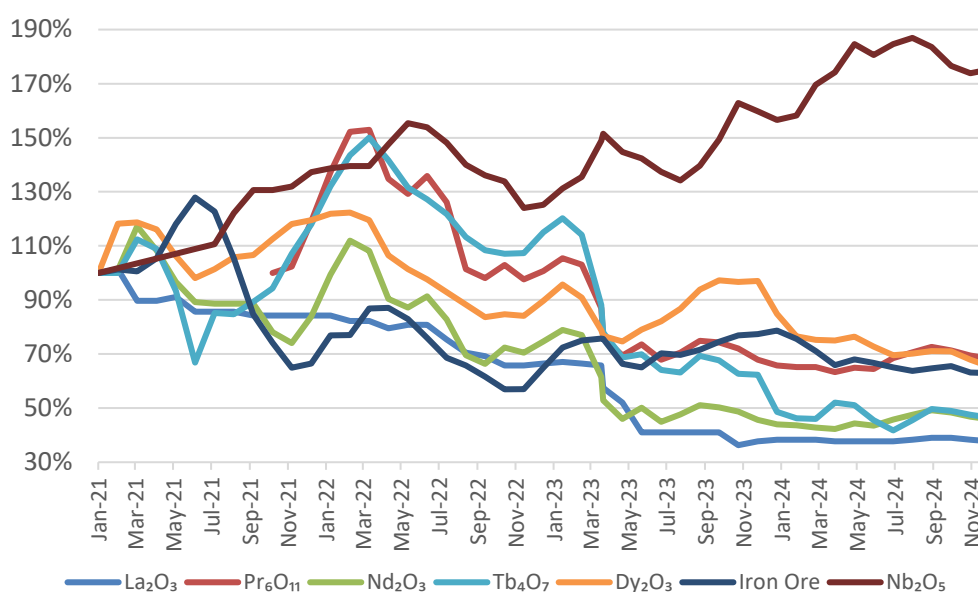


Figure 1: Monthly REO, iron ore and niobium oxide prices in relation to January 2021 [36].

Table 2: Price information averaged per year, normalized to the lanthanum oxide price [36].

|   | 2021 | 2022 | 2023 | 2024 |
|---|------|------|------|------|
| La <sub>2</sub> O <sub>3</sub>                  | 1    | 1    | 1    | 1    |
| Pr <sub>6</sub> O <sub>11</sub>                 | 83.5 | 106  | 108  | 116  |
| Nd <sub>2</sub> O <sub>3</sub>                  | 101  | 109  | 109  | 115  |
| Tb <sub>4</sub> O <sub>7</sub>                  | 1329 | 2020 | 1932 | 1514 |
| Dy <sub>2</sub> O <sub>3</sub>                  | 328  | 347  | 498  | 504  |
| Iron ore  | 0.14 | 0.12 | 0.19 | 0.22 |
| Niobium oxide (Nb <sub>2</sub> O <sub>5</sub> ) | 26.4 | 36.6 | 61.9 | 95.7 |

Table 3: Price information for 3-year averages, normalized to the lanthanum oxide price [36].

|   | 2021-2023 | 2022-2024 | % difference |
|---|-----------|-----------|--------------|
| La <sub>2</sub> O <sub>3</sub>                  | 1         | 1         | 0%           |
| Pr <sub>6</sub> O <sub>11</sub>                 | 99.1      | 109       | 11%          |
| Nd <sub>2</sub> O <sub>3</sub>                  | 106       | 110       | 4.3%         |
| Tb <sub>4</sub> O <sub>7</sub>                  | 1760      | 1821      | 3.5%         |
| Dy <sub>2</sub> O <sub>3</sub>                  | 391       | 449       | 15%          |
| Iron ore  | 0.15      | 0.18      | 19%          |
| Niobium oxide (Nb <sub>2</sub> O <sub>5</sub> ) | 41.6      | 64.7      | 55%          |

Table 3 shows price information for the same products as in Table 2, but averaged over two different 3-year periods, 2021–2023 and 2022–2024. Even when considering these three-year averages, deviations up to 19% and 55% can be observed for iron ore and niobium oxide.

In this study, across both supply routes, data is needed for in total 18 co-products – 15 REOs, iron oxide, niobium oxide and ammonium chloride. Few reports or websites provide data for all these outputs over a 10-year period, making it necessary to scan multiple sources and combine price data. There are challenges with using multiple price data sources, since detailed information is often lacking about if and how different sources handle their statistics with respect to inflation adjustments, exchange rates or for averaging over different markets. This is the case for all three main price data sources used for this study, i.e., Business Analytiq [36], the Mineral Commodity Summaries of the U.S. Geological Survey [37], and Scrap Monster [38]. As already hinted in Table 2 and Table 3, since lanthanum oxide prices are easily accessible in all three sources for all months and years that constitute reference periods, the solution found is that all the price data that originally was collected in USD/kg is normalized to the price for lanthanum oxide for each time step before calculating yearly or multiple year averages.

For ytterbium oxide, no historic data at all could be found, so the spot market price for January 2025 was used to represent the 2024 price. And to estimate the ytterbium oxide prices for 2021–2023, an average factor for an observed trend in price decrease for all REOs during that period was applied to the 2024 price. Thulium oxide prices could not be found for in any of the sources, which indicates that it is not traded at all. Consequently, its allocation factor is assigned value zero. While it was possible to find prices for all of the other of the 15 REOs for the past four years, gaps became more apparent when searching 5–10 years back. No historical price data before 2021 was found for holmium oxide, erbium oxide, thulium oxide, ytterbium oxide or lutetium oxide. These REOs make up about 4.9% of the total REO content in the ionic clays, but they are not present in the Bayan Obo mixed ore. As a result, allocation factors for the 10-year period of 2015–2024 are only applied for the Bayan Obo route.

Price data for niobium pentoxide is not available in the U.S. Geological Survey’s Mineral Commodity Summaries [37], which serves as the primary source for historical prices for 2015–2020. However, it was possible to establish a correlation between the prices for niobium ferrite and niobium pentoxide, to estimate

average yearly prices for the latter during the desired time range. A similar issue arose with the historical price data for ammonium chloride. In this case, given its low normalized price and an observation that the prices of all studied commodities were relatively stable from 2015 to 2020, the normalized price for ammonium chloride was approximated for these years and set to 0.115.

Finally, by combining the price data gathered and composition of the ores for the two supply routes studied, reported in Table 1, allocation factors can be calculated according to Equation 1. For each step in the product chain where co-products are separated, the full set of established allocation factors summarize to 1, meaning that each allocation factor corresponds to the share of the value coupled to each co-product at that stage. In further calculations, for example when assigning burdens per kilogram for individual REOs, e.g., neodymium and dysprosium as input to the magnet fabrication, each REO allocation factor is then normalized to its mass fraction in the ore, to establish specific multiplication factors.

Figure 2 shows the value distribution per kilogram of mixed REO for a number of selected time periods that also correspond to the different sets of allocation factors used for the climate impact assessment of individual REOs and complete magnets. Both REO supply routes are investigated for averages during 2021, 2021–2023, 2022–2024 and 2024, while only the Bayan Obo mixed ore route is also investigated for the 10-year average, i.e. 2015–2024. It can be noted that while Table 1 reports that cerium oxide accounts for roughly 50% of the mass fraction in the REO concentrate from the Bayan Obo mixed ore, the chart shows that it only accounts for about 2% of the value. Lanthanum oxide, samarium oxide, ytterbium oxide, holmium oxide and thulium oxide are grouped together, marked as “Rest”, since their individual value shares stay below 1.5% during all time periods under consideration. The total value for all five is below 1% for the Bayan Obo route and below 2.3% for the ion-adsorption clay route, in all cases.

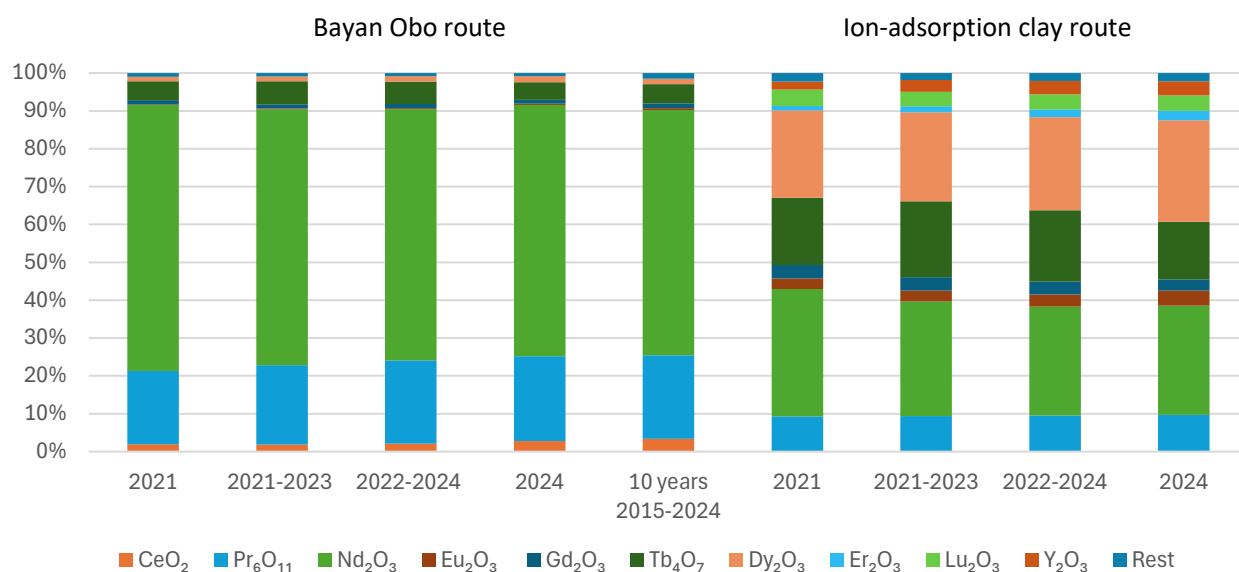


Figure 2: Value distribution in 1 kg of mixed REOs, for selected time periods and supply routes that are subject to allocation.

## 6 Climate impact results

Figure 3 and Figure 4 shows the contributions to global warming (GWP100) for praseodymium oxide and neodymium oxide, and terbium oxide and dysprosium oxide, respectively, for the two studied supply routes. Comparing the two figures, it can be noted that praseodymium oxide and dysprosium oxide display similar patterns for all time periods, but also that despite different trends across the different time periods, neodymium oxide and praseodymium oxide causes largely similar burdens, especially for the 10-year price average for the Bayan Obo route and the 3-year periods for both supply routes. This means replacing

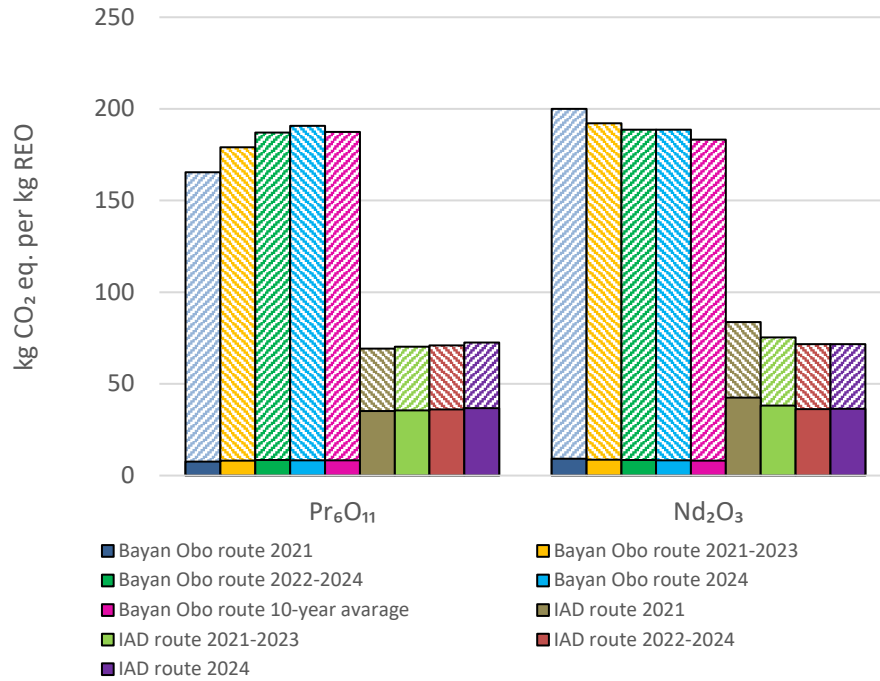


Figure 3: Contributions to global warming (GWP100) for praseodymium oxide and neodymium oxide from the Bayan Obo mixed ore supply route and the ion-adsorption clay deposit supply route, using allocation factors calculated over the selected time periods. Solid fill represents mining and beneficiation steps. Pattern fill represents remaining steps until separation.

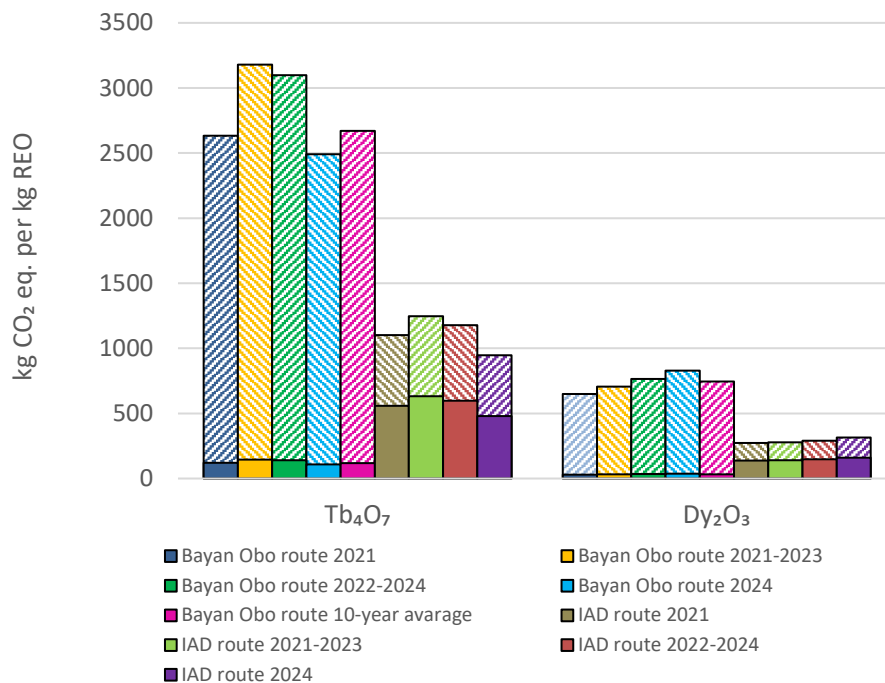
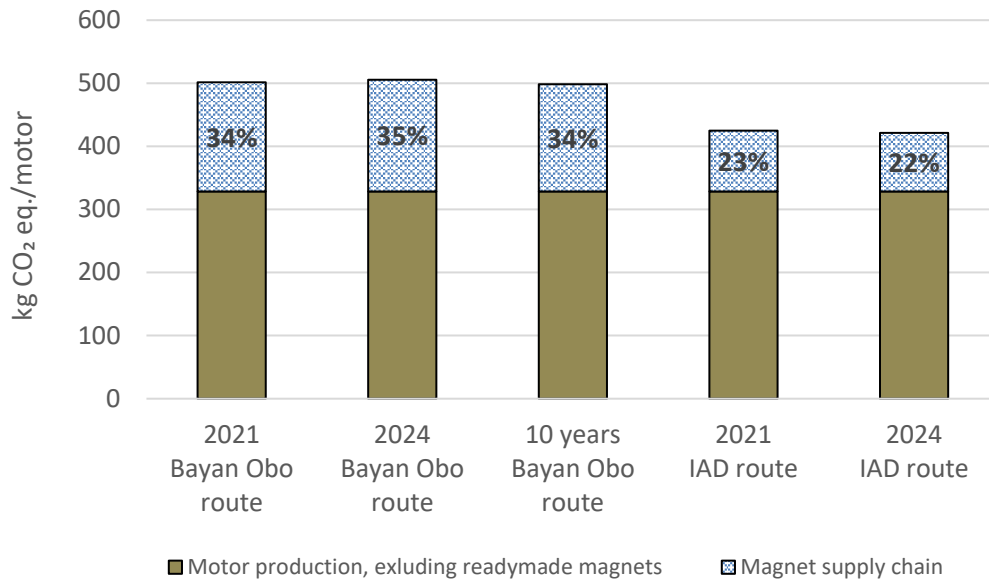


Figure 4: Contributions to global warming (GWP100) for terbium oxide and dysprosium oxide from the Bayan Obo mixed ore supply route and the ion-adsorption clay deposit supply route, using allocation factors calculated over the selected time periods. Solid fill represents mining and beneficiation steps. Pattern fill represents remaining steps until separation.





*Figure 5: Contributions to global warming (GWP100) for complete e-motors (at factory gate) with neodymium-dysprosium-iron-boron magnets, and the share of burden caused by the magnet supply route depending on the time period for the economic allocation.*

neodymium with praseodymium in the magnet body will not cause any significant change to the carbon footprint of the input REO input. To the contrary, Figure 4 clearly shows that the higher prices of terbium compared to dysprosium gives higher global warming contributions, meaning that from a climate impact point of view, this is not a preferred substitution.

Furthermore, it can be observed that the main difference in the contributions to global warming derives from the selection of the supply route. The most important part of the explanation is the overall lower total greenhouse gas emissions from the ion-adsorption clay route compared to the Bayan Obo mixed ore route, but to some extent it also depends on the fact that a slightly smaller share of the total REO value goes to the four reported REOs in the ion-adsorption clay case, as indicated by patterns shown in the value distribution of Figure 2. Another interesting detail is the generally low share of burden for the mining and beneficiation steps in the Bayan Obo mixed ore route. It offsets the effect of the combined price peak for iron ore and niobium oxide in 2024 – see Table 2 – when about 10% of the burden is allocated to these two commodities instead of the REOs. This share is otherwise in-between 5–8%.

Figure 5 shows the results on the motor level for the two studied REO supply routes when the impacts of neodymium and dysprosium present in the set of magnets are allocated based on the 2021 and 2024 averages, and then for the Bayan Obo mixed ore route also when the allocation is based on the 10-year average. In all five cases, it is assumed that neodymium and dysprosium are supplied to the subsequent magnet making from the same REO supply route. At this level, it is evident that the results are dominated by the choice of supply route, rather than the effect of the economic allocation procedure. In 2021, when the neodymium oxide contribution to global warming reaches its peak in Figure 3, this is partly balanced back by low dysprosium oxide contributions for the same year. In 2024, when both neodymium oxide and dysprosium oxide have price peaks according to Table 2, the the Bayan Obo route reaches its highest impact while the ion-adsorption clay route point in the other direction and display its lowest impact. However, both shifts are very small compared to the 2021 and 10-year averages.

## 7 Conclusions

The study shows that the choice of modelled REO supply route is the most important factor for the contributions to global warming for REEs relevant for EV e-motors. This is shown on the REO level as well as on the complete e-motor level. However, the large variation in burden between terbium oxide and

dysprosium oxide due to the price-based allocation indicates that the selection of REE for thermal stabilization matters, with dysprosium performing better than terbium over all studied time periods. On the other hand, changes in the magnet composition where the share of dysprosium is shifted up at the expense of the neodymium share would lead to a similar effect, with increased total burdens on the magnet level. Other than that, the economic allocation causes little variation of the results on the complete e-motor level, and it can be concluded that the difference between yearly averages and the 10-year average is minor, even when results vary on the REO level.

## References

- [1] Steffen, W., et al., *Planetary boundaries: Guiding human development on a changing planet*. Science, 2015. **347**(6223).
- [2] Hawkins, T.R., et al., *Comparative Environmental Life Cycle Assessment of Conventional and Electric Vehicles*. Journal of Industrial Ecology, 2013. **17**(1): p. 53-64.
- [3] Nordelöf, A., et al., *Environmental impacts of hybrid, plug-in hybrid, and battery electric vehicles—what can we learn from life cycle assessment?* The International Journal of Life Cycle Assessment, 2014. **19**(11): p. 1866-1890.
- [4] Sen, B., et al., *Material footprint of electric vehicles: A multiregional life cycle assessment*. Journal of Cleaner Production, 2019. **209**: p. 1033-1043.
- [5] Nordelöf, A., et al., *Life cycle assessment of permanent magnet electric traction motors*. Transportation Research Part D: Transport and Environment, 2019. **67**: p. 263-274.
- [6] Binnemans, K., et al., *Rare-Earth Economics: The Balance Problem*. JOM, 2013. **65**(7): p. 846-848.
- [7] Qiu, Y. and S. Suh, *Economic feasibility of recycling rare earth oxides from end-of-life lighting technologies*. Resources, Conservation and Recycling, 2019. **150**: p. 104432.
- [8] European Commission, *Proposal for a regulation of the European Parliament and of the Council establishing a framework for ensuring a secure and sustainable supply of critical raw materials and amending Regulations (EU) 168/2013, (EU) 2018/858, 2018/1724 and (EU) 2019/1020*. 2023, Official Journal of the European Union: Luxembourg, Luxembourg.
- [9] European Commission. *Questions and Answers on the Critical Raw Materials Act*. European Commission - Questions and answers 2024 [cited 2024 28th November]; Available from: [https://ec.europa.eu/commission/presscorner/detail/en/qanda\\_24\\_2749](https://ec.europa.eu/commission/presscorner/detail/en/qanda_24_2749).
- [10] Koltun, P. and A. Tharumarajah, *Life Cycle Impact of Rare Earth Elements*. ISRN Metallurgy, 2014. **2014**: p. 10.
- [11] Gupta, C.K. and N. Krishnamurthy, *Extractive Metallurgy of Rare Earths*. Minerals & Metallurgical Processing. 2005, Boca Raton, Florida: CRC Press.
- [12] ISO, *ISO 14044:2006 — Environmental management — Life cycle assessment — Requirements and guidelines*. 2006, International Organization for Standardization: Geneva, Switzerland. p. 46.
- [13] Bailey, G., et al., *Review and new life cycle assessment for rare earth production from bastnäsite, ion adsorption clays and lateritic monazite*. Resources, Conservation and Recycling, 2020. **155**: p. 104675.
- [14] Wang, Y., et al., *Physicochemical reaction-based allocation for the resource consumption of hydrometallurgical processing of rare-earth oxides—a case study on ion adsorption-type rare-earth oxides in China*. The International Journal of Life Cycle Assessment, 2025. **30**(2): p. 235-250.
- [15] Zaines, G.G., et al., *Environmental Life Cycle Perspective on Rare Earth Oxide Production*. ACS Sustainable Chemistry & Engineering, 2015. **3**(2): p. 237-244.
- [16] Arshi, P.S., E. Vahidi, and F. Zhao, *Behind the Scenes of Clean Energy: The Environmental Footprint of Rare Earth Products*. ACS Sustainable Chemistry & Engineering, 2018. **6**(3): p. 3311-3320.
- [17] Vahidi, E. and F. Zhao, *Environmental life cycle assessment on the separation of rare earth oxides through solvent extraction*. Journal of Environmental Management, 2017. **203**: p. 255-263.
- [18] Lee, J.C.K. and Z. Wen, *Rare Earths from Mines to Metals: Comparing Environmental Impacts from China's Main Production Pathways*. Journal of Industrial Ecology, 2017. **21**(5): p. 1277-1290.
- [19] Schulze, R., et al., *Developing a Life Cycle Inventory for Rare Earth Oxides from Ion-Adsorption Deposits: Key Impacts and Further Research Needs*. Journal of Sustainable Metallurgy, 2017. **3**(4): p. 753-771.
- [20] Schreiber, A., J. Marx, and P. Zapp, *Life Cycle Assessment studies of rare earths production - Findings from a systematic review*. Science of The Total Environment, 2021. **791**: p. 148257.
- [21] Nordelöf, A., et al., *A scalable life cycle inventory of an electrical automotive traction machine—Part I: design and composition*. The International Journal of Life Cycle Assessment, 2018. **23**(1): p. 55-69.

- [22] Nordelöf, A. and A.-M. Tillman, *A scalable life cycle inventory of an electrical automotive traction machine—Part II: manufacturing processes*. The International Journal of Life Cycle Assessment, 2018. **23**(2): p. 295-313.
- [23] Nordelöf, A., et al., *A Scalable Life Cycle Inventory of an Electrical Automotive Traction Machine – Technical and Methodological Description, version 1.01*. 2017, Department of Energy and Environment, Divisions of Environmental Systems Analysis & Electric Power Engineering, Chalmers University of Technology: Gothenburg, Sweden.
- [24] Li, Y.-k., et al., *Geology and mineralization of the Bayan Obo supergiant carbonatite-type REE-Nb-Fe deposit in Inner Mongolia, China: A review*. China Geology, 2023. **6**(4): p. 716-750.
- [25] Jin, H., et al., *Evaluated Utilization of Middle–Heavy REE Resources in Bayan Obo Deposit: Insight from Geochemical Composition and Process Mineralogy*. Minerals, 2025. **15**(3): p. 212.
- [26] Sprecher, B., et al., *Life Cycle Inventory of the Production of Rare Earths and the Subsequent Production of NdFeB Rare Earth Permanent Magnets*. Environmental Science & Technology, 2014. **48**(7): p. 3951-3958.
- [27] Lee, J.C.K. and Z. Wen, *Pathways for greening the supply of rare earth elements in China*. Nature Sustainability, 2018. **1**(10): p. 598-605.
- [28] Peiró, L.T. and G.V. Méndez, *Material and Energy Requirement for Rare Earth Production*. JOM - The Journal of The Minerals, Metals & Materials Society 2013. **65**(10): p. 1327-1340.
- [29] Packey, D.J. and D. Kingsnorth, *The impact of unregulated ionic clay rare earth mining in China*. Resources Policy, 2016. **48**: p. 112-116.
- [30] Qifan, W., et al. *The use and management of norm residues in processing Bayan Obo ore in China in The Sixth International Symposium on Naturally Occurring Radioactive Material (NORM VI)*. 2010. Marrakesh, Morocco: International Atomic Energy Agency.
- [31] Waggitt, P.W. *A global overview of NORM residue remediation and good practice*. in *The Sixth International Symposium on Naturally Occurring Radioactive Material (NORM VI)*. 2010. Marrakesh, Morocco: International Atomic Energy Agency.
- [32] Marx, J., et al., *Comparative Life Cycle Assessment of NdFeB Permanent Magnet Production from Different Rare Earth Deposits*. ACS Sustainable Chemistry & Engineering, 2018. **6**(5): p. 5858-5867.
- [33] Lucas, J., et al., *Rare Earths - Science, Technology, Production and Use 2015*, Amsterdam, Netherlands: Elsevier B.V.
- [34] Catena-X, *Catena-X Product Carbon Footprint Rulebook*. 2024, Catena-X Automotive Network e.V: Berlin, Germany. p. 61.
- [35] Santero, N. and J. Hendry, *Harmonization of LCA methodologies for the metal and mining industry*. The International Journal of Life Cycle Assessment, 2016. **21**(11): p. 1543-1553.
- [36] Business Analytiq. *Pricing*. 2025 [cited 2025 April]; Available from: <https://businessanalytiq.com/>.
- [37] U.S. Geological Survey. *Mineral Commodity Summaries*. 2025 [cited 2025 April]; Available from: <https://www.usgs.gov/centers/national-minerals-information-center/mineral-commodity-summaries>.
- [38] Scrap Monster. *Metal Prices*. 2025 [cited 2025 April]; Available from: <https://www.scrapmonster.com/>.

## Presenter Biography



Anders Nordelöf is Professor of Environmental Systems Analysis at the Swedish National Road and Transport Research Institute, VTI. He also works part-time as lecturer and researcher at Chalmers University of Technology. On behalf of Chalmers, Anders Nordelöf is theme leader for the research area Environment & Society within the Swedish Electromobility Center, a national Swedish competence center for electromobility. He obtained his PhD degree and docent level appointment at Chalmers and has a background as a Business Area Manager at Consat AB, an engineering bureau based in Gothenburg.